3D IMAGE REGISTRATION AND FUSION TOOLS IN SIMULATING TUMOR EVOLUTION

E. I. Zacharaki, G. K. Matsopoulos, K. S. Nikita, G. S. Stamatakos

Department of Electrical and Computer Engineering, National Technical University of Athens, Greece
e-mail: ezachar@biosim.ntua.gr

Abstract

In this paper, a three-dimensional (3D) image registration scheme along with fusion tools is developed and incorporated within a model simulating tumor growth and response to radiotherapy. This biosimulation model attempts to predict and visualize in three dimensions the in vivo tumor behavior. The necessary information for the initialization and the adjustment of the model can be provided from different medical examinations. The present study focuses on the development and evaluation of a technique that enables input information provided from different medical imaging modalities to be efficiently exploited by tumor growth simulation algorithms through the registration and fusion of computed tomography (CT) or positron emission tomography (PET) to magnetic resonance imaging (MRI) data.

Keywords

registration, fusion, tumor, simulation model, irradiation

1. Introduction

Current treatment planning algorithms are based on the concept of physical optimization of the dose distribution and rely on rather crude biological models of tumor and normal tissue response. Such algorithms practically ignore the highly complicated dynamic behavior of malignant cells and tissues. The introduction of advanced biosimulation methods based on cell proliferation mechanisms as well as on information drawn from the cellular and molecular properties of each individual malignancy and each individual patient is expected to substantially improve the radiation therapy efficiency. Novel tumor growth and response to irradiation simulation algorithms have been presented in [1]. The information required to initialize the developed biosimulation model is provided by different medical examinations. The combined exploitation of detailed three-dimensional (3D) representations of anatomy, pathology and function is achieved by applying a 3D registration and fusion scheme.

In this paper, the application of 3D registration methods to tomographic data of the brain is presented, in order to provide input to a tumor simulation model. As the simulation model is quite general, i.e. the cytokinetic and radiobiological properties of any particular type of tumor cells can provide input to the computer simulation, the registration method should be able to succeed in the majority of solid tumor growth cases. Registering intermodal medical images is a tedious process, since the identification of points correspondence between the two images is sometimes a difficult task. Moreover, the presence of characteristic edges cannot be used as a prerequisite for the registration. Therefore, an automatic registration method is proposed, in this paper, for registering multimodal medical images, which does not require any user intervention. The automatic registration method is based on the maximization of mutual information. Maximization of a similarity metric based on information theory, such as mutual information, has been demonstrated to be a very powerful criterion for multimodal medical image registration [2][3][4][5]. However, the presence of many local maxima during the iterative process poses a problem in finding a close starting estimate. The methodological novelty of the proposed approach lies on an assembly of algorithms determining in real execution time an initial guess of the final solution and reducing the risk to converge toward a misleading maximum.

The paper starts with a brief description of the *in silico* tumor evolution. Since a detailed description of the growth model can be found in [1], emphasis is put only on information input requirements based on various medical imaging modalities. Next, a spatial registration scheme is introduced and several image processing tools for fusing the registered images are presented.

2. The in silico model of tumor growth and response to irradiation

The assumptions that follow pertain to the *in vivo* simulation model developed by our research group [1]. As a first step, the imaging data (e.g. CT, MRI, PET slices), including the definition of the tumor contour and the anatomical structures of interest, the histopathologic (e.g. type of tumor) and the genetic data of the patient are

appropriately collected. In the case of radiotherapy, the distribution of the radiation dose in the region of interest, as computed during the treatment planning procedure, is also acquired.

A set of rules for the cell division and interaction behavior is adopted in which a tumor cell when cycling passes through the phases G_1 (gap 1), S (DNA synthesis), G_2 (gap 2) and M (mitosis) [6]. The adopted cytokinetic model is shown in Fig.1.

The description of the biological activity of the tumor is implemented by introducing the notion of the "geometrical cell". The anatomical region of interest is quantized in geometrical cells. Each geometrical cell belonging to the tumor contains a number of biological cells "residing" in various phases within (G_1, S, G_2, M) or out of the cell cycle (resting phase G_0, Necrosis N, Apoptosis A). The number of biological cells constituting each phase class is initially estimated according to the position of the geometrical cell within the tumor and the metabolic activity in the local area (e.g. based on PET, functional MRI). Both necrotic and apoptotic cell death are taken into account. The mechanical properties of the surrounding tissue are also taken into account in a rather simple way (e.g. absolute lack of deformability in the bone).

In case that radiotherapy treatment is delivered, the response of each cell to irradiation (Fig.1) is described by the Linear Quadratic model [6]. The radioresistance of the cells depends on the cell phase they reside.

The geometrical mesh covering the anatomic area of interest is scanned every T units of time. For each phase class of a given geometrical cell, behavior algorithms based on the cell cycle phase duration of the tumor cells, the distance from the external boundary of the tumor, the Linear Quadratic model, the genetic data of the tumor determine the updated state. Random number generators are used in order to simulate the statistical nature of various phenomena.

According to the above described process, the 3D tumor evolution is simulated. In case that radiotherapy treatment has been prescribed, the distribution of the absorbed dose (e.g. in Gy) in the region of interest is also provided to the biosimulation software in order to "predict" the most likely spatio-temporal response of the tumor.

3. The image registration method

In the specific application addressed here, image registration is of interest for the following three tasks. The first task concerns the knowledge of the dose distribution within the tumor and the surrounding tissues. In radiotherapy treatment planning, for both external radiation and brachytherapy, the dose calculation is usually based on the CT images. On the other hand, the delineation of a target volume is more precisely performed in the MR images. If registration is achieved, the coordinates of the tumor from the MR scans are

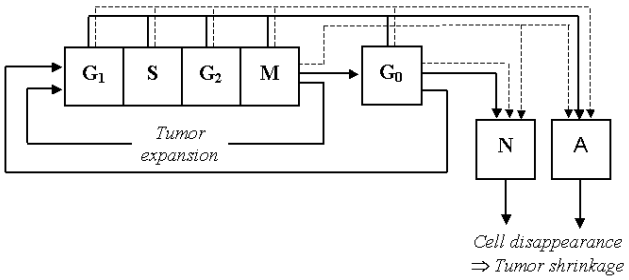

Fig. 1. Cytokinetic model of a tumor cell. The solid lines represent the transition of a cell into the various phases during tumor growth. The dashed lines represent the tumor cell response to irradiation.

transferred into the CT stereotaxy. Thus, the physical dose distribution, as calculated from the treatment planning system, can be transferred to the MR images. This combined information can be fed to the simulation model in order to predict the response of each individual cell to irradiation. This case pertains mostly to the simulation of brachytherapy, which is characterized by inhomogenous dose distributions, especially in classical intracavitary treatment. The simulation of some treatment methods of external beam radiation therapy (i.e. IMRT) could be performed assuming high homogenous dose to the tumor and ignorable dose to the surrounding healthy tissues [1].

The second task related with the application of image registration techniques for the needs of the biosimulation model refers to the quantization of the anatomical region of interest. A specialized doctor can delineate the clinical boundary of the tumor and often its necrotic area based on the corresponding MR imaging data. However the information about the metabolic activity (and therefore the density of the tumor vasculature) is usually available only through PET or functional MR images. Thus, the definition of the contours of areas corresponding to the different cell phases by the specialist with sufficient accuracy requires successful alignment of multimodal medical images.

In contrast to the above described image registration tasks referring to spatial registration, the third task pertains to temporal registration of images of the same modality in order to follow up the impact of therapy over time.

This paper focuses on spatial registration of the multimodal imaging data, as the problem of monomodal registration is less complex, but the methodology proposed may be adjusted to the temporal registration as well. An automatic registration method has been developed, which has been evaluated on CT to MR examinations. The automatic method has also been tested in the case of PET to MR registration. The preliminary results have shown that the accuracy of automatic registration involving CT was superior as compared with that of registration involving PET. Based on these results, the automatic method should be properly modified for the case of registering PET to MR data.

3.1 Methodology

A fully automatic two-step procedure for CT-to-MR registration applying rigid-body transformation is developed. If the scanner calibration problems and the problems of geometric distortions have been minimized, the rigid transformation is the most convenient for 3D scans of the head. The rigid-body transformation is represented by three translations and three rotations along the x, y and z axes. The three scaling factors are directly calculated with the voxelsize ratio of the reference image I_R and the floating image I_F [2]. In such a case, the floating image is resampled using trilinear interpolation. The choice of a 6-parameter rigid-body transformation is based on the results of a comparative study in brain imaging [7]. According to this study, the accuracy and the success rate in the case of a 6-parameter rigid-body transformation is higher than in the case of a 9-parameter rigid-body transformation. In addition, the 6-parameter transformation is twice as fast than the 9-parameter transformation.

STEP I.

In the first step, a seeded region-growing algorithm is used to automatically extract the head from the image volumes [8]. Two thresholds are defined, a low for the MR image and a high for the CT image. If one of the modalities had been PET or SPECT, the object to extract would have been the brain, because the scalp is not well perceptible in these modalities.

The objects (heads) extracted from the CT and the MR image are shaped similarly and they may be registered approximately by applying a principal axes transformation (PAT) [9]. First, the centers of mass of the two objects are aligned for translational correction ($dx, dy, dz,$). Then, the rotational errors are eliminated by rotating the objects around the center of mass (r_x, r_y, r_z). For this purpose, the eigenvectors of the covariance matrix of the objects are computed, which specify the direction of the axes of each object reference system. The eigenvectors are computed by applying the Jacobi method [10] since the covariance matrix is symmetric. The direction of the axes of the extracted 3D objects is not dependent on the object's exact outer surfaces. On the contrary, the application of a surface-matching algorithm would require to investigate the impact of the segmentation step.

While the application of the PAT method in image data of the head leads to a satisfactory approximation for the rotation around the y axis (r_y) and the translation in x- and y-direction (dx, dy), it fails to approximate well the translation along the z axis (dz) of the objects, because the clinical acquired images overlap only partially. For this reason, an exhaustive search along the z axis with offset of 50 mm around the estimated dz value is performed, in order to enhance the matching by maximizing the cross correlation of the segmented (binary) images. The cross correlation (*CC*) is a suitable matching criterion for binary images concerning both accuracy and speed performance. The cross correlation is defined as

$$CC = \frac{\sum_{x,y,z}[I_F(x,y,z)-\bar{I}_F][I_R(T(x,y,z))-\bar{I}_R]}{\sqrt{\sum_{x,y,z}[I_F(x,y)-\bar{I}_F]^2}\sqrt{\sum_{x,y,z}[I_R(T(x,y,z))-\bar{I}_F]^2}}$$

where $\bar{I}_F$ and $\bar{I}_R$ are the mean values of the unregistered image I_F and the reference image I_R respectively and *T(x,y,z)* is the transformation computed by principal axes combined with the z-tranlation vector. As the only parameter optimized over is dz, the binary images are subsampled with a subsampling factor of 2 along the x and y axes.

The other transformation parameters (dx, dy, r_x, r_y, r_z) are kept constant, as determined by the PAT method.

STEP II.

The rigid body transformation parameters obtained from the previous step are used as starting estimates for the second step of the procedure, which involves registering images I_F and I_R by maximizing the mutual information (*MI*) using local optimization techniques:

$$MI = \sum_{k=0}^{G-1}\sum_{l=0}^{G-1} p_{I_F I_R}(k,l)\log_2\frac{p_{I_F I_R}(k,l)}{p_{I_F}(k)p_{I_R}(l)}$$

where *0…G-1* is the intensity range, $p_{I_F I_R}(k,l)$ is the joint probability distribution and $p_{I_F}(k)$, $p_{I_R}(l)$ are the probability distributions of the overlapping volume of images I_F and I_R. The joint probability distribution is constructed by rigidly transforming samples in the floating image into samples in the reference image. Equal distance of the samples in the three axes has been used. Trilinear interpolation has been applied to compute the voxel intensity in the reference image [11].

Two optimization methods, namely the Powell's method [10] and the Downhill Simplex method [10] have been investigated, using as initial guess the vector of the estimated parameters in step I. Powell's method was chosen as it has been proved more precise than any other optimization methods for *MI*-based image registration [3]. The initial evaluation order of the parameters was $dx, dy, r_z, dz, r_x, r_y$ [3]. The set of directions is not reinitialized to the basis vectors during the optimization procedure. The fractional tolerance in the function value is 10^{-4}.

4. Fusion Process

A fusion process has been developed and applied following the registration process. The fusion process is independent from the selected registration method. As a single optimal way of fusing registered images does not exist, different image processing tools have been developed, allowing the user to select the most appropriate ones. Thus, various tools enabling both visual assessment of the registration achieved and combination of the complementary information are available. The slices of the reference and the transformed data sets are displayed side by side with a cursor pointing to corresponding voxels.

Checkerboard images can be produced with alternate blocks of voxels displaying image data from each modality [12]. If the user sets the blocksize equal to one pixel, the individual pixels cannot be distinguished, resulting in effective fusion of the two datasets. If a larger blocksize is selected, the registration result can be evaluated by checking the continuity of the edges.

Another tool combines anatomical structures or regions of interest in one image, i.e. it displays all image pixels, which are above a user-defined threshold (e.g. 550HU), with the color from the CT image, and the remaining pixels with the color from the MR image.

Furthermore, color overlay techniques are used to generate helpful displays. One modality is displayed using a colormap while the other is displayed on an intensity scale.

5. Results

The experiments were performed on seven patients data sets. Each patient data set consisted of a CT image and three MR images (PD, T1, T2), as well as three corrected for static field inhomogeneity MR images (PDrect, T1rect, T2rect) provided by J.M. Fitzpatrick [13]. For each patient data set, the CT image was registered to the MR images using the MR image as the reference image, resulting in 41 registration experiments in total (the T1rect image was not available for one patient). All images are axial and their characteristics are summarized in Table I. The CT images were subsampled in the axial plane to yield the same image size as the MR image, thus increasing the execution speed. All images were converted from 16-bit to 8-bit format by rescaling the intensity values to the range of 0-255. In this case, the maximum joint histogram size was 256×256. The total execution time was approximately 3 minutes on an AMD Athlon XP 1800 and depends actually only on step II, as step I of the registration method performs in real time.

In order to evaluate the registration accuracy, the stereotactic registration solution provided by the RREP project [13] was used as a reference. The error was evaluated by the root-mean-square (rms) distance between the reference and the computed transformation at eight points near the brain surface. Ground truth was obtained using bone-implanted skull markers. The traces of the stereotactic markers and the frame were removed from the images before registration. The median registration errors (in mm) for all patients' datasets for each MR-modality are shown in Table II.

Table I.
Image characteristics

Image	Num. Voxels	Voxel size (mm^3)
CT	512^2×(27-34)*	0.65^2×4.00
PD	256^2×(20-26)	1.25^2×4.00
T1	256^2×(20-26)	1.25^2×4.00
T2	256^2×(20-26)	1.25^2×4.00
PDrect	256^2×(20-26)	$(1.25\text{-}1.27)^2$×(4.00-4.12)
T1rect	256^2×(20-26)	$(1.25\text{-}1.27)^2$×(4.00-4.12)
T2rect	256^2×(20-26)	$(1.25\text{-}1.27)^2$×(4.00-4.12)

*before subsampling

The results demonstrate that the median errors show subvoxel accuracy with respect to the stereotactic registration solution without any user interaction or prior knowledge about the gray-value content of the CT and MR images. Registration differences without subvoxel accuracy (5-20 mm) have been observed in 5 (out of 41) experiments. The influence and the importance of the rescaling of the intensities and the subsampling of the CT images on the registration success should be further investigated, although it seems not to deteriorate the optimization behavior.

Following image registration, fusion tools can be used to provide helpful displays. As the registration of CT and MR images serves mostly in transferring the dose distribution calculated in the CT stereotaxy into the MR image, the fusion of the images itself does not seem to be necessary in accordance to the biosimulation model. The only case where fusion of CT and MR images shows interest for the model is when the tumor is near to bone that is not perceptible in the MR image. The bone is a structure of interest because it sets the restriction to the simulated tumor not to grow in this direction. On the contrary the registration of MR and PET images is performed in order to fuse the different image modalities and highlight the metabolic activity. Therefore the following example (Fig. 2) reveals to the fusion of MR and PET datasets, using color overlay techniques described in Section C. The external surface of the tumor is visible in the MR image, whereas the necrosis is identifiable only in the thresholded PET image. Furthermore, as demonstrated in the fused image the

Table II.
Median Errors (in mm) of the Automatic Registration Method

PD	T1	T2	PDrect	T1rect	T2rect
3.05	2.59	3.00	1.93	1.99	2.09

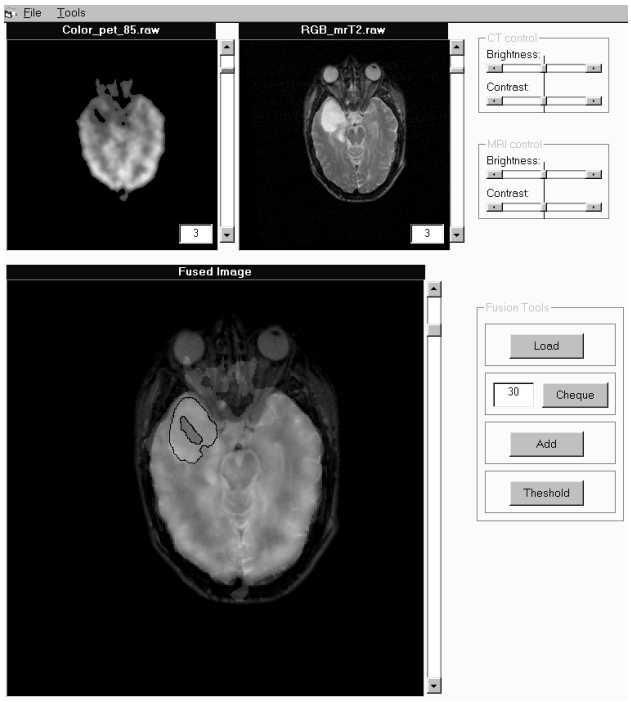

Fig. 2. The thresholded registered PET (left) and the MR-T2 (right) datasets are displayed on top. The fused image is displayed zoomed on bottom.

metabolic activity of the viable part of the tumor is inhomogeneous. The higher the metabolic activity the greater is assumed the ratio of the proliferating cells. The total tumor seems to be inactive, which means that the majority of the tumor cells are necrotic.

6. Conclusions

A 3D registration and fusion scheme was presented in order to combine information from multimodal medical data used to provide input to a 3D tumor growth simulation model for the purpose of radiotherapy optimization. By performing virtual *insilico* experiments based on the 3D simulation model, significant insight into the biological mechanisms involved in tumor growth can be gained. Furthermore, by providing the simulation model with the distribution of the absorbed radiation dose in the region of interest through the definition of a common CT-MR coordinates system, the prediction of tumor response to radiotherapy becomes more reliable.

7. Acknowledgement

Evangelia Zacharaki duly acknowledges the financial support of the Hellenic State Scholarship's Foundation.

References

[1] G.S. Stamatakos, D.D. Dionysiou, E.I. Zacharaki, N.A. Mouravliansky, K.S. Nikita, and N.K. Uzunoglu, In Silico Radiation Oncology: Combining Novel Simulation Algorithms with Current Visualization Techniques, *Proceedings of the IEEE*, *90*(11), 2002, 1764-1777.

[2] P.A. Viola and W.M. Wells III, Alignment by maximization of mutual information, *International Journal of Computer Vision*, *24*(2), 1997, 137-154.

[3] F.Maes, D. Vandermeulen, P. Suetens, Comparative evaluation of multiresolution optimization strategies for multimodality image registration by maximization of mutual information, *Medical Image Analysis*, *3*(4), 1999, 373-386.

[4] M. Holden, D.L.G. Hill, E.R.E. Denton, J.M. Jarosz, T.C.S. Cox, T. Rohlfing, J. Goodey, and D.J. Hawkes, Voxel similarity measures for 3-D serial MR brain image registration, *IEEE Trans. on Medical Imaging*, *19*(2), 2000, 94-102.

[5] P. Thevenaz and M. Unser, Optimization of mutual information for multiresolution image registration, *IEEE Trans. on Image Processing*, *9*(12), 2000, 2083-2099.

[6] G. Steel, *Basic Clinical Radiobiology* (London, UK: Arnold, 1997).

[7] J.L. Bernon, V. Boudousq, J.F. Rohmer, M. Fourcade, M. Zanca, M. Rossi, D. Mariano-Goulart, A comparative study of Powell's and Downhill Simplex algorithms for a fast multimodal surface matching in brain imaging, *Computerized Medical Imaging and Graphics*, *25*(4), 2001, 287-297.

[8] J.C. Russ, *The Image Processing Handbook* (CRC Press, 1992).

[9] N.M. Alpert, J.F. Bradshaw, D. Kennedy, J.A. Correia, The principal axes transformation – a method for image registration, *Journal of Nuclear Medicine*, *31*(10), 1990, 1717-1722.

[10] W. Press, B. Flannery, S. Teukolsky, and W. Vetterling, *Numerical recipes in C, the art of scientific computing*, *2nd edition* (Cambridge: Cambridge University Press, 1994).

[11] J.P.W. Pluim, J.B.A. Maintz, and M.A. Viergever, Interpolation artefacts in mutual information-based image registration, *Computer vision and Image Understanding*, *77*(2), 2000, 211-232.

[12] D.L.G. Hill, D.J. Hawkes, Z. Hussain, S.E.M. Green, C.F. Ruff and G.P. Robinson, Accurate combination of CT and MR data of the head: validation and applications in surgical and therapy planning, *Computerized Medical Imaging and Graphics*, *17*, 1993, 357-363.

[13] J.M. Fitzpatrick, Evaluation of Retrospective Image Registration, NIH Project Nr.1 R01 NS33926-01, Vanderbilt University, Nashville, TN.